© 2021 The Authors
756

Water Practice & Technology Vol 16 No 3
doi: 10.2166/wpt.2021.035

Utilization of hydrochar derived from waste paper sludge through hydrothermal liquefaction for the remediation of phenol contaminated industrial wastewater

Sanette Marx* and Karina van der Merwe

DST/NRF Research Chair in Biofuels and Other Clean Alternative Fuels, Centre of Excellence in Carbon-based Fuels, Faculty of Engineering, North-West University, Private Bag X6001, Potchefstroom 2520, South Africa

*Corresponding author. E-mail: sanette.marx@nwu.ac.za

Abstract

Hydrothermal liquefaction derived hydrochar produced from industrial paper sludge was used as an adsorbent to remove phenol derivatives from an industrial wastewater stream. Removal efficiency for phenol was determined using synthetic solutions (10–150 ppm) using batch adsorption experiments at a constant solution pH (8), temperature (25 ± 2 °C) and rotary speed (150 rpm). The adsorption of phenol onto hydrochar followed a Freundlich isotherm and could be described with pseudo-second-order kinetic models. Analysis of the adsorption mechanisms showed that particle film mass transport was the rate-determining step in the adsorption process. A COD removal efficiency of 31 ± 1% was achieved for the industrial wastewater stream. All phenol components in the wastewater stream could be removed, but not all organic acids and cyclic ketones. The performance of the paper sludge-based hydrochar compared well with that of activated carbon (44% COD removal). The final phenol concentration in the wastewater stream was below the acceptable phenol concentration for industrial effluents (1 mg/L). The results show that paper sludge can be converted to a valuable marketable commodity that could reduce waste management costs for a paper mill, while also reducing the cost of expensive adsorbents.

Key words: adsorption, hydrochar, hydrothermal liquefaction, paper sludge, phenol, wastewater

Highlights

- Industrial paper sludge waste was successfully converted to effective bio-adsorbent.
- HTL-based biochar was used as adsorbent without any pretreatment.
- 77.83% COD removal from industrial wastewater could be obtained.
- Final total phenol concentration was below 1 ppm.
- Bulk fluid mass transfer was the rate determining step in the adsorption process.

INTRODUCTION

Phenol and phenol derivatives are well-known for their toxicity to all forms of life as well as being non-biodegradable and bio-accumulative (Zhou *et al.* 2017; Wong *et al.* 2018). Therefore, the

Water Practice & Technology Vol 16 No 3
doi: 10.2166/wpt.2021.035

maximum allowable phenolic content in potable water and industrial effluent must be lower than 1 μg/L and 1 mg/L respectively (Tabassi *et al.* 2017). The most common methods used to treat industrial wastewater are adsorption, chemical precipitation, membrane filtration solvent extraction, ion-exchange, flotation and electrocoagulation (Aziz *et al.* 2008; Ariffin *et al.* 2017). Although these methods have been proven to be efficient in removing organic pollutants, the associated high operating cost and low efficiency when low contaminant concentrations are present outweigh their operational feasibility (Aziz *et al.* 2008; Barakat 2011). The high cost of adsorption can, however, be lowered if less expensive adsorbents, compared to activated carbon, could be found. Recent literature has reported on the use of hydrochar as such an adsorbent (Tan *et al.* 2015).

Hydrochar is a solid coal-like product that is produced from the thermal decomposition of biomass waste by employing either pyrolysis or HTL (Gollakota *et al.* 2018), with HTL being favoured because of the transitional structure of the hydrochar and the many oxygenated functional groups and mineral compounds, which promote adsorption, present on the hydrochar surface (Saleh *et al.* 2016). Various studies have reported on the production of pyrolysis-derived hydrochar as an adsorbent from waste materials such as pine waste (Amerkhanova *et al.* 2017), paper mill sludge (Yoon *et al.* 2017), sugarcane bagasse (Wong *et al.* 2018) and papaya peels (Abbaszadeh *et al.* 2016). However, limited literature is available on the use of industrial waste such as paper sludge for the production of hydrochar adsorbents through HTL for the removal of organic and inorganic pollutants from industrial wastewater streams.

Paper sludge is a waste product from the pulp and paper industry and approximately 300–350 million tons per of paper sludge is produced annually (Ioelovich 2014), the disposal cost of which amounts to approximately 60% of the total plant operating cost (Hojamberdiev *et al.* 2008; Gurram *et al.* 2015). The application of this waste product for the production of affordable adsorbents will lower the environmental impact of landfilled paper sludge and reduce the operating costs for paper mills. A study on the use of paper sludge-based hydrochar produced via pyrolysis for removal of fluoxetine from synthetic and real solutions (Jaria *et al.* 2015) showed no correlation between the surface area of the hydrochar and the adsorption capacity. Furthermore, activating agents added to the sludge prior to pyrolysis did not significantly improve the adsorption properties of the produced hydrochar. The effectiveness of pyrolysis-derived paper sludge-based hydrochar to remove phosphate and methylene blue from synthetic solution were investigated by Hojamberdiev *et al.* (2008) and it was reported that maximum multifunctional adsorption capacity of 0.11 mmol/g was observed with a maximum hydrochar surface area of 70 m^2/g. Furthermore, phosphate was removed as Ca-phosphate that precipitated on the surface of the hydrochar. Méndez *et al.* (2009) found that de-inking paper sludge leads to mesoporous material during pyrolysis while paper sludge from virgin pulp mills forms microporous materials. Both materials were used to adsorb Cu^{2+} from wastewater. It was found that the de-inking sludge-based hydrochar had a higher adsorption capacity, which was ascribed by the authors to a higher Ca and Mg exchange content, a higher concentration of oxygenated functional groups on the surface and the larger pore size facilitating easy diffusion transport compared to the mesopores of the virgin sludge-based hydrochar.

To date, most of the studies that produced paper sludge-based hydrochar employed pyrolysis rather than hydrothermal liquefaction (HTL). The latter is better suited to the processing of wet feedstock compared to pyrolysis and operates at milder process conditions. Also, the adsorption performance of paper sludge-based hydrochar produced from HTL for the removal of phenolic compounds from industrial wastewater has not previously been reported. Therefore, in this study, the removal of phenol from industrial wastewater using HTL-derived hydrochar from industrial paper sludge was investigated. Isotherms were drawn to determine the mechanism of adsorption for the individual components and pseudo-second-order kinetic models were used to determine design parameters for

Water Practice & Technology Vol 16 No 3
doi: 10.2166/wpt.2021.035

industrial application. Mass transfer analysis elucidated the rate-determining step of the adsorption process.

MATERIALS AND METHODS

Paper sludge and industrial wastewater

Paper sludge was collected from an industrial paper recycling plant in South Africa at a point after the wastewater treatment and dewatering activities. The mill utilizes both bleached hardwood virgin fibres and recycled fibres as feedstock. Industrial wastewater was collected from the same paper mill at a point after the primary water treatment step. Activated carbon, used as a baseline, was procured from Associated Chemical Enterprises (ACE), South Africa. Both the paper sludge and industrial wastewater were stored at 4 °C after collection until used.

Hydrochar preparation from paper sludge

An SS316 batch autoclave with a working volume of 945 mL was filled with approximately 200 g of paper sludge without the addition of water as the paper sludge already contained sufficient water for the HTL reactions to proceed. The autoclave was pressurized to an initial pressure of 0.50 MPa at room temperature and heated to 300 °C at a rate of 3.42 °C/min, where it was kept constant for 15 min before the reactor was allowed to cool naturally and the hydrochar was recovered from the reactor via filtration. The filtered hydrochar was washed with enough acetone to remove all residual bio-oil components. The clean hydrochar was then dried overnight at 105 °C to a moisture content below 10% and stored in airtight containers until used as adsorbents.

Physicochemical characterization

The paper sludge, hydrochar, and activated carbon were characterized by proximate, elemental and Fourier-transform infrared spectroscopy (FTIR) analysis. The surface morphology was studied by energy-dispersive X-ray (EDX) analysis. The surface area and mineralogy of the hydrochar and activated carbon samples were determined by Brunauer–Emmett–Teller (BET) and X-ray diffraction (XRD) and X-ray fluorescence (XRF) analysis, respectively. The point of zero charge analysis was done by standard methods. Compositional analysis of the paper sludge was done through fibre analysis according to the Van Soest method (Van Soest 1963). The average particle size of the produced hydrochar was determined by a Hydro 2000 MU Malvern Mastersizer.

Wastewater characterization

The collected wastewater was characterized by measuring the pH, conductivity, chemical oxygen demand (COD), total phenol content, 5-day biological oxygen demand (BOD_5), total dissolved solids (TDS), total suspended solids (TSS), calcium content and total phenolic content. The pH was measured using a Metrohm 692 pH meter and conductivity was measured with an EDT Instruments FE 280 conductivity meter. COD was determined by a photo spectrometric method using a test kit (Macherey – Nagel 100–1500 ppm COD test kit) (analogous to the DIN 150 15705-H45, EPA 4104, APHA 5220 D and DIN 38409-H-41-1 standard methods). BOD_5 analysis was outsourced to an accredited wastewater testing laboratory that used the W044-43-W reference method for BOD analysis according to the DIN EN 25813-G21 standard BOD testing method. TDS and TSS were determined according to the SANS 6049:2010 and SANS 5213:2013 methods respectively. Calcium concentration was determined using an ICP-OES instrument. The total phenolic content was

Water Practice & Technology Vol 16 No 3
doi: 10.2166/wpt.2021.035

determined using a standard test kit (Merck 0.002–5 ppm phenol test kit) (method analogous to the EPA 420.1, APHA 5530 C and D, ISO 6439 and ASTM D1783-01 standard for determination of phenol in wastewater).

Batch adsorption experiments

Adsorption experiments were performed in 250 mL glass Duran bottles, using 100 mL adsorbate solution with an initial pH of 8. All the sample bottles were closed once the experiment was started. The pH of the solutions was adjusted by adding either 0.1 M HCl or 0.1 M NaOH solutions, dropwise. Sample bottles were continuously shaken at a rotary speed of 150 rpm in a Labcon platform incubator shaker at 25 ± 2 °C. Samples taken during the synthetic and industrial wastewater experiments were filtered with 0.22 μm Grafiltech and 0.45 μm Pall GHP membrane syringe filters respectively.

The effect of hydrochar dosage on adsorption performance was investigated at hydrochar dosages between 2 g/L and 12 g/L. Once the optimum adsorbent dosage was determined, isotherms and kinetic experiments were performed at initial phenol concentration of between 10 and 150 ppm. The effect of the presence of calcium as a contaminant during phenol adsorption was done at an initial phenol concentration of 10 ppm and a calcium (as $Ca(NO_3)_2$ $4H_2O$) concentration of 600 ppm. The phenol concentration was quantified by an Agilent Technologies 1260 Infinity II high-performance liquid chromatography (HPLC) instrument fitted with an InfinityLab Poroshell 120 EC-C18 column (4.6 × 100 mm and 4 μm with column ID). The HPLC had two mobile phases namely: A – 1% formic acid in water and 1% formic acid in acetonitrile, mixed initially: 92% A, 8% B, and at 10 minutes: 70% A, 30% B. The column temperature was set as 40 °C. An injection volume of 10 μL was used with a Diode Array Detector with a wavelength of 275 nm and a bandwidth of 4 nm. Quantification of phenol components was done using a standard set of calibration curves. The detection and quantification limits for phenol were 2.67 μg/L and 8.9 μg/L respectively.

Data analysis

The adsorption capacity at time t can be calculated by Equation (1) (Zhang *et al.* 2016).

$$q_t = \frac{V_{sol}(C_i - C_t)}{m} \tag{1}$$

where q_t is the instantaneous adsorption capacity at time t (mg/g), C_i is the initial adsorbate concentration (ppm), C_t is the instantaneous residual adsorbate concentration in the solution at time t (ppm), V_{sol} is the volume of the solution (L) and m is the mass of the adsorbent used (g). Once equilibrium is reached, the removal efficiency of the adsorption process can be calculated as shown by Equation (2) (Rout *et al.* 2016).

$$\textit{Removal Efficiency}\ (\%) = \frac{C_i - C_e}{C_i} \times 100 \tag{2}$$

The equilibrium data were interpreted by fitting Langmuir and Freundlich isotherms and Henry's law isotherms to the data.

The Langmuir isotherm model is given by Equation (3) (Liu *et al.* 2010).

$$\frac{1}{q_e} = \frac{1}{K_L\, q_{max} C_e} + \frac{1}{q_{max}} \tag{3}$$

where q_{max} is the maximum adsorption capacity and K_L is the Langmuir constant related to the free

Water Practice & Technology Vol 16 No 3
doi: 10.2166/wpt.2021.035

energy of adsorption (L/mg). The Freundlich isotherm model is given by Equation (4) (Hameed *et al.* 2008; Abbaszadeh *et al.* 2016).

$$\ln(q_e) = \ln(K_F) + \left(\frac{1}{n}\right) \ln(C_e) \tag{4}$$

where K_F is an indicator of the adsorption capacity ($mg^{(1-1/n)}/(L^n.g)$ and $(1/n)$ is the adsorption intensity or the favourability of the adsorption process. Henry's law is given by Equation (5) (Tran *et al.* 2017).

$$q_e = K_H C_e \tag{5}$$

where K_H is known as Henry's constant or distribution coefficient (L/mg). Furthermore, the kinetic data was interpreted by fitting both kinetic (pseudo-first-order and pseudo-second-order rate expressions) and diffusional models (intra-particle and film diffusion models) to the experimental data. The linearized form of the pseudo-first-order rate model is shown in Equation (6) (El-Naas *et al.* 2010).

$$\ln(q_e - q_t) = \ln(q_e) - k_1 t \tag{6}$$

where k_1 is the pseudo-first-order rate constant (1/min). The linearized form of the pseudo-second-order rate model is given by Equation (7) (Dursun *et al.* 2005).

$$\frac{t}{q_t} = \frac{1}{k_2 q_e^2} + \frac{t}{q_e} \tag{7}$$

where k_2 is the pseudo-second-order rate constant (g/(mg.min)). Furthermore, the calculated parameters can then be used to determine the initial rate of adsorption, h_o as shown by Equation (8).

$$h_o = k_2 q_e^2 \tag{8}$$

RESULTS AND DISCUSSION

Characterization of paper sludge, hydrochar and activated carbon

The compositional analysis of the paper sludge showed that it consisted of cellulose (34.88 wt. %), hemicellulose (12.03 wt.%), lignin (24.53 wt.%), cutin (14.05 wt.%), protein (2.25 wt.%) and fat by ether extract (1.01 wt.%). The large lignin content of the sludge (22.54%, dry basis) was attributed to the presence of corrugated boxes in the feed to the paper recycling plant, which contain lignin to improve the stiffness of the boxes (Antonides 2000).

A hydrochar yield of 723 ± 84 g/kg (dry basis) was obtained at a reaction temperature of 300 °C, which was comparable to the hydrochar from paper sludge yield of 640 g/kg reported by Jaria *et al.* (2015) at 800 °C under pyrolysis conditions. Some physical characteristics of the paper sludge, hydrochar, and activated carbon are given on a dry basis (db) in Table 1.

The BET analysis showed a relatively low microporous (1.54 m^2/g) and mesoporous surface area (24.78 m^2/g) for the hydrochar compared to un-activated pyrolysis-based hydrochar surface areas reported in the literature (Hojamberdiev *et al.* 2008; Méndez *et al.* 2009; Jaria *et al.* 2015; Yoon *et al.* 2017). The activated carbon had a large micro-and mesoporous surface area of 550.45 m^2/g and 277.72 m^2/g. Proximate analysis showed the presence of ash species in the hydrochar (41 ± 4 wt. %, db)

Water Practice & Technology Vol 16 No 3
doi: 10.2166/wpt.2021.035

Table 1 | Elemental and proximate analysis (wt. %, db) and BET surface area

	Paper sludge	Hydrochar	Activated carbon
Carbon (C)	35.1	39	83
Hydrogen (H)	4.7	3.5	0.2
Nitrogen (N)	0.37	0.44	0.003
Oxygen (O)[a]	60	58	15
Moisture	55 ± 2.2	2 ± 0.5	6.4 ± 2
Volatile matter	70 ± 0.7	42 ± 1	6.7 ± 0.7
Ash	22 ± 0.7	41 ± 4	2.3 ± 0.7
Fixed carbon	7.9 ± 0.5	16 ± 2	91 ± 0.5
BET surface area (m^2/g)			
Mesoporous		1.54	277.72
Microporous		24.78	550.45

[a]Determined by difference.

originating from the paper sludge that was also rich in mineral-based species (22 ± 0.7 wt. %, db). EDX analysis revealed that the mineral-based particles were mostly calcium, silicon and aluminium. XRD analysis indicated that the main mineral constituent of the hydrochar was calcite (CaO), identified by the sharp narrow peaks at $2\theta = 27°$, 34.2°, 42°, 46.1°, 50.6°, 55.2°, 55.9°, 57°, 67.9° and 76.8°. The presence of a small amount of kaolinite ($Al_2Si_2O_5(OH)_4$) was indicated by narrow peaks produced at $2\theta = 14.2°$ and 28.9°. XRF analysis validated the distribution of mineral constituents in the hydrochar to be calcite (47.68%), quartz (27.23%) and aluminium oxide (18.50%). Calcium carbonate ($CaCO_3$) was observed in the FTIR spectra of the paper sludge as a sharp peak at a wavelength of 876 cm^{-1} and the sharp peaks at wavelengths of 1,032 cm^{-1}, 3,619 cm^{-1} and 3,694 cm^{-1} were assigned to kaolinite. During HTL, $CaCO_3$ decomposes to CaO, which explains the origin of CaO in the hydrochar. FTIR spectra of the hydrochar also showed the presence of many oxygenated functional groups that can act as adsorption sites.

Effect of hydrochar dosage

The point of zero charge analysis showed that the point of zero charge of the hydrochar was close to 8. Since the pH of the industrial wastewater used in this study was also close to 8, all experiments were performed at a fixed pH of 8. The effect of the hydrochar dosage on phenol adsorption is shown in Figure 1. The increase in effective surface area with an increase in adsorbent dosage from 2 g/L to 12 g/L led to an expected increase in removal efficiency as more active sites create more opportunities for the adsorption of phenol molecules.

The overall adsorption capacity, however, decreased initially from 3.16 mg/g to 1.51 mg/g as a higher dosage resulted in an increase in the amount of unsaturated active sites while the number of phenol molecules in the solution remained the same (Abbaszadeh *et al.* 2016). At hydrochar dosages of above 6 g/L, the hydrochar particles started forming agglomerates due to overcrowding, which resulted in some active adsorption sights being masked and thus no increase in adsorption capacity was observed (Gholizadeh *et al.* 2013; Xu *et al.* 2013). A dosage of 12 g/L was chosen to use in further studies to limit the effect of the experimental error on the results.

Adsorption isotherms

Adsorption isotherms obtained from equilibrium adsorption data is necessary for the design of adsorption systems (Figure 2).

Water Practice & Technology Vol 16 No 3
doi: 10.2166/wpt.2021.035

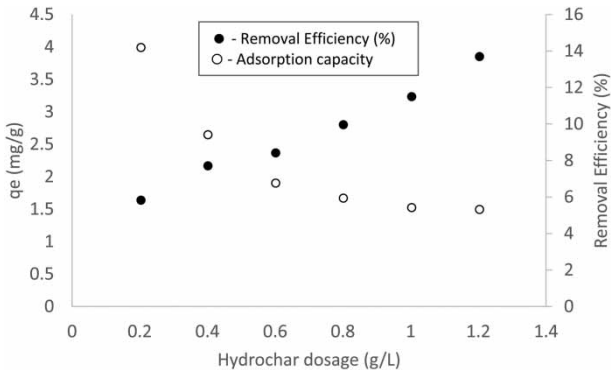

Figure 1 | Effect of hydrochar dosage on phenol removal efficiency and adsorption capacity.

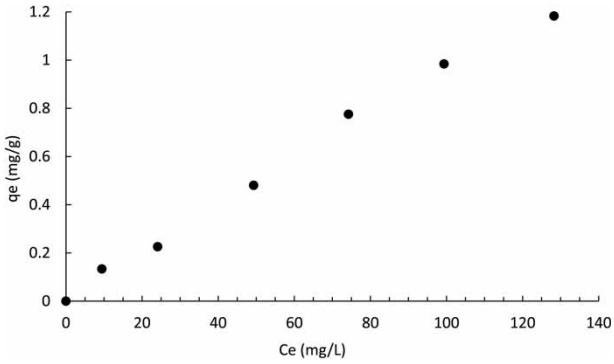

Figure 2 | Adsorption isotherm of phenol onto hydrochar.

The equilibrium isotherm in Figure 2 conforms to a class L (normal Langmuir) isotherm (Bonilla-Petriciolet *et al.* 2013), which is typically found for adsorption in aqueous media. Langmuir type isotherms imply that adsorption capacity is directly proportional to the phenol concentration in the aqueous medium until the adsorption sites become limited and molecules start competing for available sites. Furthermore, Langmuir type isotherms indicate that molecules are adsorbed flat on the surface and binding between the molecules and active sites are through weak Van der Waals forces, i.e. physical adsorption (Bonilla-Petriciolet *et al.* 2013). Further classification of the isotherm as a subclass 4 isotherm indicates the formation of a fresh adsorption surface as seen by the slight change in the slope of the isotherm at an equilibrium phenol concentration of approximately 74 mg/L. The latter can be explained by molecule-molecule interactions on the surface, resulting in fresh adsorption sites. The corresponding parameters calculated for each isotherm model at a 95% confidence level are given in Table 2.

From the accuracy of fit, it can be seen that the data were best described by the Freundlich isotherm. The constants, K_F and n in the Freundlich isotherm is related to the macroscopic behaviour of the adsorption system and the microscopic behaviour of the molecules being adsorbed (Yang 1998). A heterogeneity factor (n) larger than 1 indicates adsorption onto a heterogeneous surface through physical adsorption. The Freundlich isotherm has also been associated with multilayer adsorption and molecule-molecule interactions, which confirms the isotherm classification as a subclass 4 Langmuir type isotherm. Adsorption onto more than one type of active site was confirmed with FTIR analysis (Figure 3).

Some changes in the spectra of the fresh and used hydrochar were observed. New peaks were observed in the spectra of used hydrochar at 2,360 cm^{-1}, the single peak at a wavelength of approximately 460 cm^{-1} split into two small weak peaks and the peak observed at approximately 400 cm^{-1}

Water Practice & Technology Vol 16 No 3
doi: 10.2166/wpt.2021.035

Table 2 | Parameters obtained from fitting the Langmuir (Equation (3)), Freundlich (Equation (4)) and Henry's law (Equation (5)) to equilibrium adsorption data for phenol onto hydrochar

	Value	Adj. R2	*P*-value
Langmuir isotherm			
K_L (L/mg)	$8.7 \times 10^{-3} \pm 1.2 \times 10^{-3}$	0.95	5.59×10^{-04}
q_{max} (mg/g)	1.7 ± 0.9	0.95	0.14
R_L	0.44–0.91		
Freundlich isotherm			
K_F ($(mg^{0.12}.L^{0.7})/g$)	$1.7 \times 10^{-2} \pm 2 \times 10^{-3}$	0.98	4.23×10^{-05}
n	$1.14 \pm 1.2 \times 10^{-3}$	0.98	8.20×10^{-05}
Henry's law			
K_H (L/mg)	$9.2 \times 10^{-3} \pm 2 \times 10^{-4}$	0.80	1.34×10^{-7}

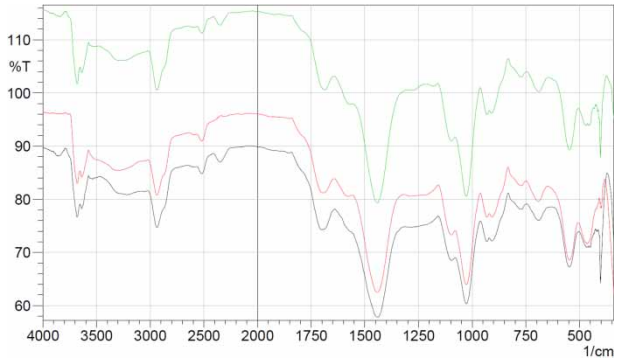

Figure 3 | Comparison of FTIR spectra of hydrochar used for the adsorption of phenol from solutions containing 10 ppm and 150 ppm with that of unused hydrochar.

increased to a large, sharp peak in the spectra of the used hydrochar. The weak peak in the spectra of the fresh hydrochar at 1,600 cm^{-1} became a shoulder in the spectra of the used hydrochar and the peaks at 1,450 cm^{-1} and 1,050 cm^{-1} were slightly larger. The peak at 2,360 cm^{-1} (H bond in –COOH (Abdel-Ghani *et al.* 2015) together with the peak at 1,050 cm^{-1} (primary alcohol C-O stretch) was assigned to the physical adsorption bonds of phenol to active carbon and ether groups on the hydrochar surface. The presence of additional phenyl groups attached to the hydrochar surface after batch adsorption is confirmed by the slight increase in absorption at 1,450 cm^{-1} (C = C-C aromatic ring stretch) and the change in the weak shoulder peak at 1,600 cm^{-1}. The FTIR analysis thus confirms adsorption onto different surface groups and thus the good fit of the Freundlich isotherm to the equilibrium adsorption data.

Adsorption kinetics

Evolution of the kinetic profile of an adsorption system is an important part of an adsorption process as it offers insight into the rate of adsorption, the residence time required to reach equilibrium conditions and the effectiveness of the adsorbent used (Bonilla-Petriciolet *et al.* 2013). The kinetic profile obtained for this study is shown in Figure 4.

The adsorption of phenol onto the hydrochar produced required between 30 and 360 min to reach equilibrium conditions. The intermediate equilibrium plateaus observed in the data for all initial phenol concentrations are attributed to adsorption of phenol molecules onto different types of active sites (as confirmed by the FTIR analysis). As one type of site is saturated, a plateau is reached

Water Practice & Technology Vol 16 No 3
doi: 10.2166/wpt.2021.035

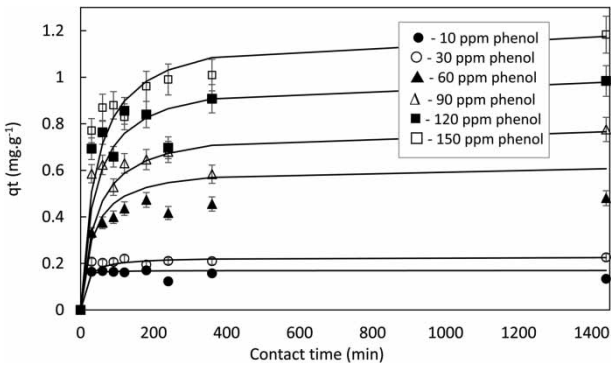

Figure 4 | Adsorption capacity as a function of time at different initial phenol concentrations.

in the adsorption capacity and another type of adsorption site is then filled, until all available sites have been saturated and true equilibrium adsorption is reached.

In order to determine the rate of adsorption of phenol onto the hydrochar produced, the pseudo-first-order and pseudo-second-order rate models were fitted to the experimental data. However, only the results of the fitting of the pseudo second-order model are given here, because the pseudo-first-order model did not fit the equilibrium data ($R^2 \leq 0$). The kinetic parameters obtained from fitting a pseudo-second-order kinetic model at a 95% confidence level are given in Table 3.

Table 3 | Pseudo-second-order fitted parameters for phenol adsorption onto hydrochar (Equation (7))

C_i (mg·L^{-1})	$q_{e,exp}$ (mg/g)	$q_{e,cal}$ (mg/g)	k_2 (g/(mg.min))	h_0 (mg/(g.min))	Adj.R^2
10	0.17	0.17	0.41 ± 0.23	0.007	0.997
30	0.23	0.23	0.32 ± 0.074	0.016	0.999
90	0.78	0.79	0.03 ± 0.070	0.019	0.993
120	0.98	1.01	0.03 ± 0.004	0.026	0.995
150	1.18	1.21	0.02 ± 0.0014	0.029	0.998

The equilibrium adsorption capacities predicted by the model correlated well with the experimental values obtained. It can be seen from Table 3 that both the specific rate of adsorption and equilibrium adsorption capacity (q_e) increases with an increase in initial phenol concentration. The initial rate of adsorption (h_0) increases as the initial phenol concentration increases and the driving force for mass transfer is increased.

Mechanism of adsorption

Adsorption isotherm and adsorption kinetics analysis has shown that more than one type of active site is involved in the adsorption process and there is a change in the mechanism of adsorption, as seen from the changes in h_0 and q_e with a change in initial phenol concentration.

A number of mass transfer steps are involved in the adsorption of a solute from an aqueous media onto a solid surface. It is assumed from the general theories of momentum and mass transfer that each adsorbent particle is surrounded by a transport film across which the concentration of the adsorbate changes from the bulk fluid to the surface of the solid. The first step in the overall adsorption process is thus the bulk diffusion of adsorbate molecules to the outer layer of the transport film surrounding the solid adsorbent particle. Molecules thus need to be transported across the particle film before attaching to the outer surface of the adsorbent, from where it can be transported through pore

Water Practice & Technology Vol 16 No 3
doi: 10.2166/wpt.2021.035

diffusion into the internal pore structure of the solid particle for adsorption onto available adsorption sites. The rate of transport in each step is a function of the adsorbate concentration and properties as well as the characteristics of the adsorbent. Mass transfer, momentum transfer and thermodynamics all play a role in determining the rate of transport during each step, but the slowest of the transport steps determines the overall rate of adsorption for a specific adsorbate. External transport is usually rate limiting when adsorbate molecules are relatively small and present at low concentrations, while internal transport is usually rate limiting for larger molecules present in higher concentrations, but the rate limiting step needs to be determined for each adsorption system. Mathematical theory to describe the different phenomena influencing adsorption is by nature complex and difficult to solve. However, it has been noted that for intra-particle transport, most solutions show a square root relationship of adsorption time with the fraction of adsorption sites occupied (Kouyoumdjiev 1992). The presence of more than one rate-determining step can thus be determined by examining the relationship between q_t and $t^{0.5}$ (Jaman *et al.* 2009). This relationship represents initial intra-particle diffusion and if the relationship shows more than one straight line, there is more than one mechanism controlling the adsorption process. From a plot of q_t and $t^{0.5}$ (Figure 5), there is one straight line relationship for an initial phenol concentration (C_0) of 10 to 30 mg/L. At C_0 of 60 mg/L, there was an initial linear relationship up to 120 minutes, followed by a plateau for the rest of the contact time.

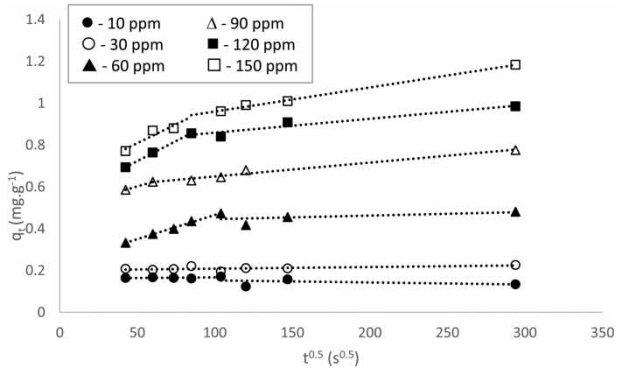

Figure 5 | Intra-particle diffusion plots for adsorption of phenol onto hydrochar at different initial phenol concentrations.

From a C_0 of 90 mg/L and higher, there was distinctly two mechanisms involved in the adsorption process, as indicated by the two straight-line sections for each C_0. The dimensionless Biot (Bi) number is an indication of the relationship between mass transfer from the bulk fluid to the surface of the adsorbent and intra-particle diffusion (Girish & Murty 2016). The adsorption process is controlled by intra-particle diffusion if the Bi number is larger than 100 and by particle film mass transfer if the Bi number is smaller than 100.

$$Bi = \frac{k_f d_p}{D_e} \tag{9}$$

where k_f is the film mass transfer coefficient, d_p is the average hydrochar particle diameter and D_e is the effective intra-particle diffusion coefficient.

The film mass transfer coefficient can be determined from a plot of C/C_0 vs time, where C is the concentration of phenol in the adsorption media at time t and C_0 is the initial phenol concentration. The effective intra-particle diffusion coefficient can be determined through a plot of $-\ln(1-F^2)$ versus time, where F is the ratio between adsorption capacity at time t (q_t) and the equilibrium adsorption capacity (q_e) (Girish & Murty 2016). The calculated k_f and D_e values at a 95% confidence level are given in Table 4. Values for 10 and 60 ppm initial concentration are not reported due to low fit of accuracy ($R^2 < 0.2$) during determination of the calculated parameters.

Water Practice & Technology Vol 16 No 3
doi: 10.2166/wpt.2021.035

Table 4 | Calculated film mass transfer coefficients and effective intra-particle diffusion coefficients

C_0 (mg/L)	$k_f \times 10^9$ (m/s)	R^2	$D_e \times 10^{16}$ (m^2/s)	R^2	Bi (–)
30	0.14 ± 0.04	0.71	2.9 ± 0.31	0.98	10.8
90	0.23 ± 0.05	0.88	34.1 ± 4.4	0.91	4.61
120	0.98 ± 0.33	0.80	54.5 ± 8.7	0.87	16.09
150	2.5 ± 0.36	0.90	376 ± 17	0.99	14.69

The values obtained for k_f and D_e are in the same order of magnitude as obtained by Girish & Murty (2016) for the adsorption of phenol onto *Lantana camera* and forest waste. The Bi numbers for all initial phenol concentrations were smaller than 100, indicating that the adsorption process was controlled by film mass transfer across all concentrations investigated. Both k_f and D_e increased exponentially with an increase in initial phenol concentration because of the increased driving force for mass transfer. The results of the study, therefore, indicate that adsorption of phenol onto hydrochar proceeded by the outer surface adsorption first, followed by pore diffusion in the mesopores and adsorption of phenol onto the internal surface of the hydrochar particles. Die values of the film diffusion coefficients (Table 6) were determined using the model presented by (Doke & Khan 2017) (Equation (10)).

$$\ln(1-F) = ln\left(\frac{6}{\pi^2}\right) - D_{film}\left(\frac{\pi^2}{r_0^2}\right)t \tag{10}$$

where r_0 is the average particle radius. The calculated film diffusion coefficients are presented in Table 5.

Table 5 | Calculated film diffusion coefficients (Equation (10))

C_0 (mg/L)	30	90	120	150
$D_{film} \times 10^{16}$ (m^2/s)	27.6 ± 0.71	36 ± 4.8	57.8 ± 9.98	1,600 ± 86

Effect of calcium on phenol adsorption

The industrial wastewater used in this study had a high calcium content that could influence the adsorption of phenol onto the hydrochar (Tabassi *et al.* 2017). The adsorption performance of hydrochar for adsorption of phenol with or without the presence of calcium is compared in Figure 6.

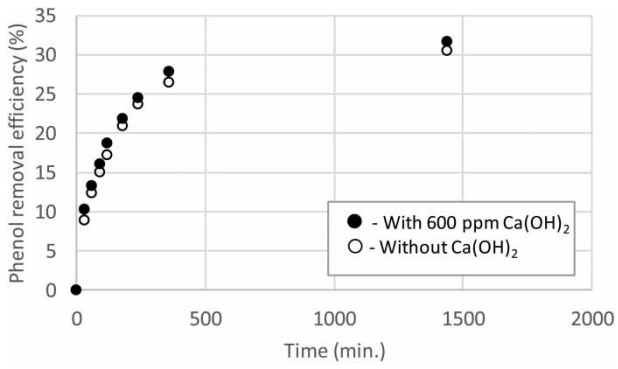

Figure 6 | Comparison of adsorption performance for removal of phenol from water containing only phenol or phenol with calcium present.

Water Practice & Technology Vol 16 No 3
doi: 10.2166/wpt.2021.035

The presence of calcium nitrate ($Ca(NO_3)_2{\cdot}4H_2O$) in the adsorption media did not have a significant effect on the removal efficiency of phenol. It is expected that the presence of dissolved salts will influence the electrostatic forces between the phenol molecules and the adsorbent surface. In this study, it was shown that the adsorption process is controlled by film mass transfer and the concentration of phenol molecules on the external surface of the hydrochar is thus expected to be low at any given time (Sobiesiak 2017). Therefore, FTIR analysis (Figure 7) was performed on the used hydrochar to determine the impact of the calcium salt on the interaction of phenol with the hydrochar.

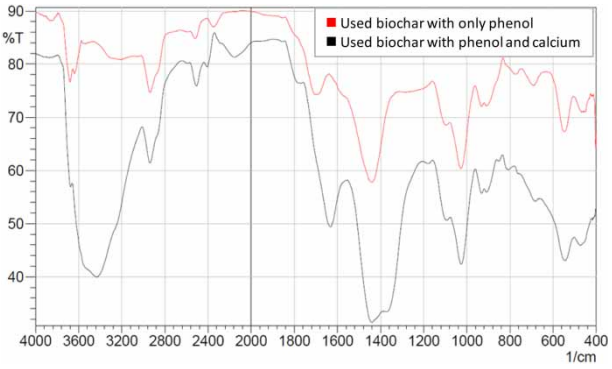

Figure 7 | Comparison of FTIR spectra of hydrochar used for adsorption of phenol from a 10 ppm solution compared to that of hydrochar used to adsorb.

The spectra for the used hydrochar in the presence of $Ca(NO_3)_2{\cdot}4H_2O$ show the typically expected peaks at 3,640 cm^{-1} (-OH group in water), 2,350 cm^{-1} together with 1,650 cm^{-1} (H_2O) and the broad double peak at 1,360–1,480 cm^{-1} (NO_3^-). The peak at 2,360 cm^{-1} that disappeared was previously shown to be one of the –COOH active sites on the hydrochar surface where phenol adsorbed. The shoulder associated with phenol adsorption onto the hydrochar surface at 1,600 cm^{-1} disappeared and the peak indicating phenol adsorption at 1,450 cm^{-1} is masked by the nitrate peak. The presence of nitrate ions thus shielded some of the preferred phenol adsorption sites, but not the extent where it negatively impacted the total phenol adsorption capacity. The slightly higher removal efficiency of phenols in the presence of the calcium salt observed in Figure 6 could be due to a slight decrease in the ionic strength of the solution due to adsorption of nitrate ions onto the hydrochar surface.

Adsorption of phenol from an industrial wastewater

Characteristic properties of collected wastewater were determined to be: COD of 2,720 mg/L, BOD_5 695 mg/L, BOD_5/COD ratio of 0.26, total phenol concentration of 16.7 mg/L, total calcium concentration of 579 mg/L, TDS of 3,794 mg/L and conductivity of 3.1 mS/cm. The wastewater had a slight alkaline pH (7.8) and a relatively high total suspended solids (TSS) concentration (320 mg/L) as expected for recycling paper mill wastewater (Pokhrel & Viraraghavan 2004; Rahman & Kabir 2010). The calculated BOD_5/COD ratio was lower than 0.4, indicating that the wastewater is not readily biodegradable and would require a tertiary treatment step to reach the effluent limits. The latter is due to the relatively high phenolic content of the wastewater. The paper mill that produced the wastewater used in this study uses recycled fibres with virgin fibres to ensure that paper products produced have increased mechanical properties. Therefore, low phenol concentrations in the wastewater are expected as most of the lignin was not broken down but contained within the desired paper products produced in the process. The high calcium concentration in the wastewater is in agreement with the calcium observed in the paper sludge.

Water Practice & Technology Vol 16 No 3
doi: 10.2166/wpt.2021.035

COD removal results

The complex composition of the wastewater and the low concentration of some compounds made a qualitative analysis of individual components difficult and, therefore, the efficiency of the hydrochar to lower the COD of the wastewater stream was used as a quantitative measure to follow the removal efficiency. The COD removal efficiency of the hydrochar was compared to that of activated carbon (the industry standard) (Figure 8).

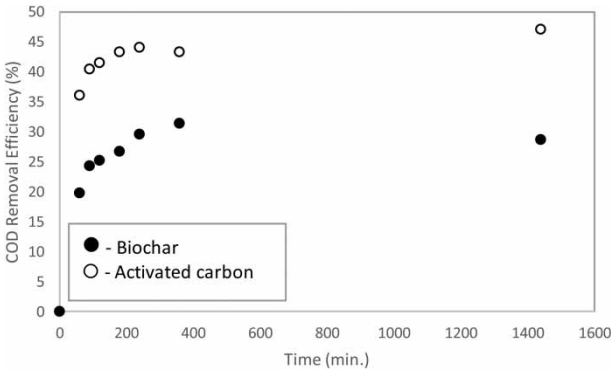

Figure 8 | Comparison of adsorption performance of hydrochar produced in this study to that of activated carbon for COD removal from industrial wastewater.

Approximately 44 ± 2% of the COD was removed by the activated carbon after 240 minutes and 31 ± 1% by the hydrochar after 360 minutes. After 24 hours, removal efficiency for the activated carbon increased slightly to 47 ± 3% and that of hydrochar decreased slightly to 29 ± 1%. The slight changes in concentration after 24 hours fall within or very close to the standard deviation in the COD measurement and were thus presumed to be the result of the normal variation in the data. The difference in removal efficiency between activated carbon and hydrochar is significant and probably the result of the much higher surface area of the activated carbon compared to that of hydrochar. The average COD removal efficiency obtained for hydrochar (~30%) and activated carbon (~41%) in this study is lower than what is reported in literature (Huggins *et al.* 2016), but higher than that reported for phenol removal using paper sludge-based biochar (Calace *et al.* 2002). Table 6 presents the phenol content of the wastewater before and after adsorption.

From Table 6, it can be seen that all the phenol derivatives were removed to a concentration below that of the detection limit of the HPLC, but only 9% of the other organic components present in the waste water were removed. These results show that hydrochar can be considered as a suitable and inexpensive adsorbent for continuous practical wastewater treatment of wastewater containing phenolic components as contaminants. Lastly, the COD removal efficiencies obtained for the hydrochar by adsorption were higher than other wastewater treatment methods such as ozonation (approximately 20%), but not aerobic treatment technologies such as aerated stabilisation basins

Table 6 | Phenol components present in wastewater before and after treatment with hydrochar

	Before (mg/L)	After (mg/L)
Hydroquinone	12	<0.045
Catechol	1	<0.008
Guaiacol	0.4	<0.006
Phenol	3.2	<0.003
Other organic components	39.8	36.2

Water Practice & Technology Vol 16 No 3
doi: 10.2166/wpt.2021.035

(67%) and bio-filters (52%) (Amat *et al.* 2005; Ashrafi *et al.* 2015). An analysis of total phenolic components in the wastewater confirmed that the COD removal observed was mostly due to the adsorption of phenolic components onto the hydrochar. The concentration of residual phenolic components in the wastewater was well below the allowable acceptable limit of 1 mg/L for phenolic compounds present in industrial effluents (World Health Organization 1994). The phenol removal efficiency obtained by the hydrochar in real industrial wastewater was slightly higher than in a synthetic wastewater environment containing only phenol. According to Calace *et al.* (2002), the adsorption of substituted phenolic compounds with a more hydrophobic nature (due to having low pKa values) will adsorb more easily than phenol with a higher solubility and therefore higher pKa value. Furthermore, an increase in the ionic strength due to the presence of inorganic salt species such as divalent calcium, magnesium, sodium and potassium has been found to promote the adsorption of organic contaminants that are more hydrophobic than phenol such as phenolic compounds substituted with additional chlorine and nitrogen-based groups.

CONCLUSIONS

In this study, it was evident that hydrochar derived from paper sludge can be used as an adsorbent to remove hazardous organic pollutants such as phenol and/or phenol derivatives from both synthetic and real industrial wastewater streams. However, low phenol removal efficiencies were obtained in synthetic phenol solutions due to the low surface area and therefore, the limited amount of active sites available on the surface of the produced hydrochar. The low surface area was largely contributed to the blockage of pores by mineral-based compounds such as calcite and kaolinite. The presence of calcium in a binary solution with phenol did not significantly influence the adsorption of phenol. The hydrochar achieved a COD removal efficiency of only $31 \pm 5.1\%$, but all phenolic components were removed from the wastewater. Therefore, it can be concluded that hydrochar derived from paper sludge through HTL has the potential to replace expensive adsorbents such as activated carbon to remove harmful organic pollutants such as phenolic components from real industrial wastewater streams. The direct usage of wet biomass waste products such as paper sludge for HTL purposes also offers cost-effective waste management solutions that reduce the environmental impact of the pulp and paper industry.

DECLARATION OF CONFLICT OF INTEREST

The authors declare that there is no conflict of interest.

FUNDING

The authors gratefully acknowledge the financial support of the Paper Manufacturers' Association of South Africa (PAMSA), Mpact and the National Research Foundation of South Africa (NRF grant UID 91635) for this research. This work is based on the research supported by the National Research Foundation. Any opinion, finding and conclusion or recommendation expressed in this material is that of the author(s) and the NRF does not accept any liability in this regard.

DATA AVAILABILITY STATEMENT

All relevant data are included in the paper or its Supplementary Information.

Water Practice & Technology Vol 16 No 3
doi: 10.2166/wpt.2021.035

REFERENCES

Abbaszadeh, S., Wan Alwi, S. R., Webb, C., Ghasemi, N. & Muhamad, I. I. 2016 Treatment of lead-contaminated water using activated carbon adsorbent from locally available papaya peel biowaste. *J. Clean. Prod.* **118**, 210–222. https://doi.org/10.1016/j.jclepro.2016.01.054.

Abdel-Ghani, N. T., El-Chaghaby, G. A. & Helal, F. S. 2015 Individual and competitive adsorption of phenol and nickel onto multiwalled carbon nanotubes. *J. Adv. Res.* **6**, 405–415. https://doi.org/10.1016/j.jare.2014.06.001.

Amat, A. M., Arques, A., Miranda, M. A. & López, F. 2005 Use of ozone and/or UV in the treatment of effluents from board paper industry. *Chemosphere* **60**, 1111–1117. https://doi.org/10.1016/j.chemosphere.2004.12.062.

Amerkhanova, S., Shlyapov, R. & Uali, A. 2017 The active carbons modified by industrial wastes in process of sorption concentration of toxic organic compounds and heavy metals ions. *Colloids Surfaces A Physicochem. Eng. Asp.* **532**, 36–40. https://doi.org/10.1016/j.colsurfa.2017.07.015.

Antonides, F. 2000 *Simultaneous Neutral Sulphite Semichemical Pulping of Hardwood and Softwood*. University of Kwa-Zulu Natal, Durban, South Africa.

Ariffin, N., Abdullah, M. M. A. B., Zainol, M. R. R. M. A., Murshed, M. F., Hariz-Zain, Faris, M. A. & Bayuaji, R. 2017 Review on Adsorption of Heavy Metal in Wastewater by Using Geopolymer. In *MATEC Web of Conferences*. https://doi.org/10.1051/matecconf/20179701023.

Ashrafi, O., Yerushalmi, L. & Haghighat, F. 2015 Wastewater treatment in the pulp-and-paper industry: a review of treatment processes and the associated greenhouse gas emission. *J. Environ. Manage.* **158**, 146–157. https://doi.org/10.1016/j.jenvman.2015.05.010.

Aziz, H. A., Adlan, M. N. & Ariffin, K. S. 2008 Heavy metals (Cd, Pb, Zn, Ni, Cu and Cr(III)) removal from water in Malaysia: post treatment by high quality limestone. *Bioresour. Technol.* **99**, 1578–1583. https://doi.org/10.1016/j.biortech.2007.04.007.

Barakat, M. A. 2011 New trends in removing heavy metals from industrial wastewater. *Arab. J. Chem.* **4**, 361–377. https://doi.org/10.1016/j.arabjc.2010.07.019.

Bonilla-Petriciolet, A., Mendoza-Castillo, D. I. & Reynel-Ávila, H. E. 2013 *Adsorption Processes for Water Treatment and Purification*. Springer, Cham, Switzerland. https://doi.org/10.1016/S0301-7036(14)70853-3.

Calace, N., Nardi, E., Petronio, B. M. & Pietroletti, M. 2002 Adsorption of phenols by papermill sludges. *Environ. Pollut.* **118**, 315–319. https://doi.org/10.1016/S0269-7491(01)00303-7.

Doke, K. M. & Khan, E. M. 2017 Equilibrium, kinetic and diffusion mechanism of Cr(VI) adsorption onto activated carbon derived from wood apple shell. *Arab. J. Chem.* **10**, S252–S260. https://doi.org/10.1016/j.arabjc.2012.07.031.

Dursun, G., Çiçek, H. & Dursun, A. Y. 2005 Adsorption of phenol from aqueous solution by using carbonised beet pulp. *J. Hazard. Mater.* **125**, 175–182. https://doi.org/10.1016/j.jhazmat.2005.05.023.

El-Naas, M. H., Al-Zuhair, S. & Alhaija, M. A. 2010 Removal of phenol from petroleum refinery wastewater through adsorption on date-pit activated carbon. *Chem. Eng. J.* **162**, 997–1005. https://doi.org/10.1016/j.cej.2010.07.007.

Gholizadeh, A., Kermani, M., Gholami, M. & Farzadkia, M. 2013 Kinetic and isotherm studies of adsorption and biosorption processes in the removal of phenolic compounds from aqueous solutions: comparative study. *J. Environ. Heal. Sci. Eng.* **11**, 1–10. https://doi.org/10.1186/2052-336X-11-29.

Girish, C. R. & Murty, V. R. 2016 Mass transfer studies on adsorption of phenol from wastewater using *Lantana camara*, forest waste. *Int. J. Chem. Eng.* **2016**. https://doi.org/10.1155/2016/5809505.

Gollakota, A. R. K., Kishore, N. & Gu, S. 2018 A review on hydrothermal liquefaction of biomass. *Renew. Sustain. Energy Rev.* **81**, 1378–1392. https://doi.org/10.1016/j.rser.2017.05.178.

Gurram, R. N., Al-Shannag, M., Lecher, N. J., Duncan, S. M., Singsaas, E. L. & Alkasrawi, M. 2015 Bioconversion of paper mill sludge to bioethanol in the presence of accelerants or hydrogen peroxide pretreatment. *Bioresour. Technol.* **192**, 529–539. https://doi.org/10.1016/j.biortech.2015.06.010.

Hameed, B. H., Tan, I. A. W. & Ahmad, A. L. 2008 Adsorption isotherm, kinetic modeling and mechanism of 2,4,6-trichlorophenol on coconut husk-based activated carbon. *Chem. Eng. J.* **144**, 235–244. https://doi.org/10.1016/j.cej.2008.01.028.

Hojamberdiev, M., Kameshima, Y., Nakajima, A., Okada, K. & Kadirova, Z. 2008 Preparation and sorption properties of materials from paper sludge. *J. Hazard. Mater.* **151**, 710–719. https://doi.org/10.1016/j.jhazmat.2007.06.058.

Huggins, T. M., Haeger, A., Biffinger, J. C. & Ren, Z. J. 2016 Granular biochar compared with activated carbon for wastewater treatment and resource recovery. *Water Res.* **94**, 225–232. https://doi.org/10.1016/j.watres.2016.02.059.

Ioelovich, M. 2014 Waste paper as promising feedstock for production of biofuel. *J. Sci. Res. Reports* **3**, 905–916. https://doi.org/10.9734/jsrr/2014/8025.

Jaman, H., Chakraborty, D. & Saha, P. 2009 A study of the thermodynamics and kinetics of copper adsorption using chemically modified rice husk. *Clean – Soil, Air, Water* **37**, 704–711. https://doi.org/10.1002/clen.200900138.

Jaria, G., Calisto, V., Gil, M. V., Otero, M. & Esteves, V. I. 2015 Removal of fluoxetine from water by adsorbent materials produced from paper mill sludge. *J. Colloid Interface Sci.* **448**, 32–40. https://doi.org/10.1016/j.jcis.2015.02.002.

Kouyoumdjiev, M. S. 1992 *Kinetics of Adsorption From Liquid Phase on Activated Carbon*. Technische Universiteit Eindhoven, Eindhoven. https://doi.org/10.6100/IR387873.

Liu, Q. S., Zheng, T., Wang, P., Jiang, J. P. & Li, N. 2010 Adsorption isotherm, kinetic and mechanism studies of some substituted phenols on activated carbon fibers. *Chem. Eng. J.* **157**, 348–356. https://doi.org/10.1016/j.cej.2009.11.013.

Water Practice & Technology Vol 16 No 3
doi: 10.2166/wpt.2021.035

Méndez, A., Barriga, S., Fidalgo, J. M. & Gascó, G. 2009 Adsorbent materials from paper industry waste materials and their use in Cu(II) removal from water. *J. Hazard. Mater.* **165**, 736–743. https://doi.org/10.1016/j.jhazmat.2008.10.055.

Pokhrel, D. & Viraraghavan, T. 2004 Treatment of pulp and paper mill wastewater – a review. *Sci. Total Environ.* **333**, 37–58. https://doi.org/10.1016/j.scitotenv.2004.05.017.

Rahman, M. M. & Kabir, K. B. 2010 Wastewater treatment options for paper mills using recycled paper/imported pulps as raw materials: Bangladesh perspective. *Chem. Eng. Res. Bull.* **14**, 65–68. https://doi.org/10.3329/cerb.v14i1.5236.

Rout, P. R., Dash, R. R. & Bhunia, P. 2016 Nutrient removal from binary aqueous phase by dolochar: highlighting optimization, single and binary adsorption isotherms and nutrient release. *Process Saf. Environ. Prot.* **100**, 91–107. https://doi.org/10.1016/j.psep.2016.01.001.

Saleh, S., Kamarudin, K. B., Ghani, W. A. W. A. K. & Kheang, L. S. 2016 Removal of organic contaminant from aqueous solution using magnetic biochar. *Procedia Eng.* **148**, 228–235. https://doi.org/10.1016/j.proeng.2016.06.590.

Sobiesiak, M. 2017 Chemical Structure of Phenols and Its Consequence for Sorption Processes. In: *Phenolic Compounds Natural Sources, Importance and Applications* (Soto-Hernández, M., Tenango, M. P. & García-Mateos, R. eds). IntechOpen, pp. 3–28. https://doi.org/10.5772/66537.

Tabassi, D., Harbi, S., Louati, I. & Hamrouni, B. 2017 Response surface methodology for optimization of phenol adsorption by activated carbon: isotherm and kinetics study. *Indian J. Chem. Technol.* **24**, 239–255.

Tan, X., Liu, Y., Zeng, G., Wang, X., Hu, X., Gu, Y. & Yang, Z. 2015 Application of biochar for the removal of pollutants from aqueous solutions. *Chemosphere* **125**, 70–85. https://doi.org/10.1016/j.chemosphere.2014.12.058.

Tran, H. N., You, S. J., Hosseini-Bandegharaei, A. & Chao, H. P. 2017 Mistakes and inconsistencies regarding adsorption of contaminants from aqueous solutions: a critical review. *Water Res.* **120**, 88–116. https://doi.org/10.1016/j.watres.2017.04.014.

Van Soest, P. 1963 Use of detergents in the analysis of fibrous feeds. II. A rapid method for the determination of fiber and lignin. *J. Assoc. Off. Agric. Chem.* **46**, 829–835. https://doi.org/10.1007/11679363_33.

Wong, S., Ngadi, N., Inuwa, I. M. & Hassan, O. 2018 Recent advances in applications of activated carbon from biowaste for wastewater treatment: a short review. *J. Clean. Prod.* **175**, 361–375. https://doi.org/10.1016/j.jclepro.2017.12.059.

World Health Organization 1994 *Phenol Health and Safety Guide, International Programme on Chemical Safety*. World Health Organization, Geneva, Switzerland.

Xu, P., Zeng, G., Huang, D., Hu, S., Feng, C., Lai, C., Zhao, M., Huang, C., Li, N., Wei, Z. & Xie, G. 2013 Synthesis of iron oxide nanoparticles and their application in *Phanerochaete chrysosporium* immobilization for Pb(II) removal. *Colloids Surfaces A Physicochem. Eng. Asp.* **419**, 147–155. https://doi.org/10.1016/j.colsurfa.2012.10.061.

Yang, C. 1998 Statistical mechanical study on the Freundlich isotherm equation. *J. Colloid Interface Sci.* **208**, 379–387. https://doi.org/10.1006/jcis.1998.5843.

Yoon, K., Cho, D. W., Tsang, D. C. W., Bolan, N., Rinklebe, J. & Song, H. 2017 Fabrication of engineered biochar from paper mill sludge and its application into removal of arsenic and cadmium in acidic water. *Bioresour. Technol.* **246**, 69–75. https://doi.org/10.1016/j.biortech.2017.07.020.

Zhang, D., Huo, P. & Liu, W. 2016 Behavior of phenol adsorption on thermal modified activated carbon. *Chinese J. Chem. Eng.* **24**, 446–452. https://doi.org/10.1016/j.cjche.2015.11.022.

Zhou, N., Chen, H., Xi, J., Yao, D., Zhou, Z., Tian, Y. & Lu, X. 2017 Biochars with excellent Pb(II) adsorption property produced from fresh and dehydrated banana peels via hydrothermal carbonization. *Bioresour. Technol.* **232**, 204–210. https://doi.org/10.1016/j.biortech.2017.01.074.

First received 17 February 2020; accepted in revised form 19 March 2021. Available online 1 April 2021